Ionic Liquids from Car−Parrinello Simulations, Part I: Liquid $AlCl_3$

Barbara Kirchner,*,† Ari P. Seitsonen,*,‡,§ and Jürg Hutter*,‡

Lehrstuhl für Theoretische Chemie, Institut für Physikalische und Theoretische Chemie, Universität Bonn, Wegelerstr. 12, D-53115 Bonn, Germany, Physikalisch-Chemisches Institut, Universität Zürich, Winterthurerstr. 190, CH-8057 Zürich, Switzerland, and Institut de Minéralogie et de Physique des Milieux Condensés (IMPMC), CNRS + Université Pierre et Marie Curie, 4 place Jussieu, case 115, F-75252 Paris, France

Received: March 5, 2006; In Final Form: April 25, 2006

The properties of isolated $AlCl_3$ clusters and the bulk system are investigated by means of static and dynamic electronic structure methods. We find important structural motifs with the edge connectivity dominant in a dimer and the corner connectivity dominant in a trimer. Furthermore, the trimer cluster exhibits an interesting ring structure with large cooperative effects relative to the dimer. Comparing the found structural motifs in isolated molecule calculations with the structure of the liquid allows us to determine the dominace of edge connectivity in the liquid. The size of the clusters present in the liquid indicates indeed that the dimer is the most abundant species, but there are also trimers, tetramers, and pentamers present. From the local dipole analysis both for the isolated clusters as well as for the liquid, further proof for the edge connectivity is given. However, all results point to the fact that there is also some small percentage of corner connectivity present that might be attributed to the most stable corner-connected cluster, namely the trimer. Importantly, we find that energetic considerations of isolated (static) clusters only do not represent the findings in liquid phase. Instead, a quantum cluster equilibrium approach or simulations are needed.

1. Introduction

Recently, new solvents and solutions have received increasing attention in chemical research because many of the materials commonly used nowadays in laboratories and in the chemical industry are considered to be unsafe for reasons of environmental protection.[1] The new solvents that are called ionic liquids are salt mixtures with melting points below the ambient temperature. In contrast to classical molten salts, which are usually melting at high temperatures, viscous and very corrosive substances, ionic liquids are fluid at low temperatures (<350 K or even at room temperature) and relatively weakly viscous.[1] Although the first ionic liquids have been known since 1929, their application as solvents in chemical reactions has increasingly gained attention only recently.[1]

$AlCl_3$ salts exhibit attractive properties such as low-temperature eutectics of possible relevance to energy storage.[2−4] The thermodynamic and physical properties of these low-melting acidic mixtures, i.e., more than 50% $AlCl_3$, show strong compositional dependences that are not completely understood. Complex ions as $AlCl_4^-$, $Al_2Cl_7^-$, and $Al_3Cl_{10}^-$ are found in these acidic mixtures, and with increasing $AlCl_3$ concentration, the proportion of $Al_2Cl_7^-$ increases. All complex ion species are essentially polymeric, built up by the same fundamental unit of $AlCl_4^-$ tetrahedra being connected with each other. However, the precise structures are not well established, and there is some disagreement concerning the structure of the Al−Cl−Al bridge in the $Al_2Cl_7^-$ species.[5−7]

Aluminum trichloride melts at a relatively low temperature (as compared to other trihalides) of 466 K, forming a liquid with a behavior typical for molecular liquids.[4,8−10] Quantum chemical calculations (refs 4, 5, 11, 12, and references therein) indicate a bent bridge in the $AlCl_3$ dimer. The established model of the molten $AlCl_3$ is that of fluid Al_2Cl_6 dimers, each formed by edge sharing of two distorted $AlCl_4^-$ tetrahedra units, which is in agreement with quantum chemical studies.[5,7,13] Inspired by the similarities between $ZnCl_2$[14] and $AlCl_3$ (both have a low melting point and a very low conductivity), the structure has been reinvestigated and a "sparse network liquid" has been suggested.[5] The liquid seems to consist of Al_2Cl_6 dimers, and it might be a liquid with reduced connectivity and strong covalent bonding. Rather than that of solely edge-sharing tetrahedral units, the measurements of the structure indicates also some percentage of corner-sharing tetrahedra in a Badyals study.[5] Later comprehensive studies employed polarizable pair potentials to obtain the structure of the liquid.[10,15] This "ionic" interaction model showed to be an accurate representation of the molecular $AlCl_3$.

In this article, we first study the $AlCl_3$ systems by means of static quantum chemical methods, which is certainly not sufficient enough to describe the condensed phase. Thus, we extend our study to Car−Parrinello[16] simulations of the condensed phase after gaining insight into the basic physics governing the gas phase or isolated molecule interaction. With the Car−Parrinello simulation technique, one is able to treat for polarization and molecular many-body effects at each simulation step, and the electronic structure is calculated on the fly. These calculations are restricted to gradient-corrected density functional theory due to the bottleneck of computer time for such simulations.

This article is the first part of an investigation of ionic liquids formed by the salts of $AlCl_3$ and is dedicated to pure liquid $AlCl_3$. The second part will be dedicated to 1-ethyl-3-methylimidazolium (C_2C_1im) chloroaluminates, i.e., C_2C_1imCl@-

* Corresponding authors. E-mail: Kirchner@thch.uni-bonn.de (B.K.); Ari.P.Seitsonen@iki.fi (A.P.S.); Hutter@pci.unizh.ch (J.H.).

† Lehrstuhl für Theoretische Chemie, Institut für Physikalische und Theoretische Chemie, Universität Bonn.

‡ Physikalisch-Chemisches Institut, Universität Zürich.

§ Institut de Minéralogie et de Physique des Milieux Condensés.

10.1021/jp061365u CCC: $33.50
Published on Web 05/24/2006

$(AlCl_3)_n$[1,17] clusters ($n = 1, 3$) up to a simulation of C_2C_1imCl in liquid $AlCl_3$.

2. Methodology and Nomenclature

2.1. Static Calculations. For the quantum chemical structure optimizations and single point calculations, we used the density functional and ab initio programs provided by the TURBOMOLE 5.1 suite.[18] We employed the gradient-corrected functional BLYP[19,20] and PBE[21] with the RI technique[22−24] and the hybrid functional B3LYP.[25,26] Moreover, we applied second-order Møller−Plesset perturbation theory (MP2) with the resolution of the identity (RI) technique.[27] The DFT results were obtained from all-electron restricted Kohn−Sham calculations. Ahlrichs' TZVP basis set has been used throughout, featuring a valence triple-ζ basis set with polarization functions on all atoms.[28] All the interaction energies were counterpoise corrected with the procedure of Boys and Bernardi[29] in order to minimize the basis set superposition errors (BSSE). They turned out to be between 2 and 5 kJ/mol per monomer for the interaction energies calculated with Ahlrichs' TZVP basis set.

For the vibrational analysis, the second derivatives of the total electronic energy were computed as numerical first derivatives of analytic energy gradients with the program SNF.[30] The vibrational frequencies and the zero-point vibrational energies ΔZPE are obtained within the harmonic approximation.

2.2. Dynamic Calculations. We performed all the dynamical calculations with the CPMD code.[31] Two gradient-corrected local density functionals for exchange and correlation, i.e., BLYP[19,20] and PBE,[21] were employed throughout, and the Kohn−Sham orbitals were expanded in a plane wave basis with a kinetic energy cutoff of 50 Rydbergs for the BLYP functional calculation and 25 Rydbergs for the PBE calculations; the higher cutoff energy with the BLYP functional was used to check convergence. In general norm-conserving pseudopotentials of the Troullier−Martins type[32] were taken with pseudization radii of s = 1.25, p = 1.55, d = 1.40 and s = 2.0, p = 1.6, d = 1.82 for aluminum and for chlorine, respectively. Core-valence interaction of aluminum and chlorine is treated by s and p potentials. The pseudopotentials were applied in the Kleinman−Bylander representation[33] with the highest angular momentum as the local potential. The Brillouin zone sampling was restricted to the Γ point, and periodic boundary conditions were applied. All Car−Parrinello simulations were performed in the microcanonical (NVE) ensemble; the total energy was conserved to within 0.033 meV/ps.

All single-molecule calculations are performed in a cubic box of 12 Å length with the PBE functional, and the fictitious electron mass was set to 1000 au while the time step was 0.148 fs. The temperature was fixed to 470 K with Nosé−Hoover thermostats[34−37] coupled to the ionic degrees of freedom. A Poisson solver that avoids periodicity[38] was used in order to avoid spurious box effects for the isolated molecule calculations.

The PBE simulation of the liquid encounters 64 aluminum chloride units. The molecules were initially placed randomly in the cubic box of 22.7 Å length, yielding a density of 1.211 g/cm^3. The fictitious electron mass was set to 1000 au and the time step was 0.148 fs. After an equilibration of several ps, data was collected from a 10 ps trajectory. In the BLYP simulation, the maximally localized Wannier functions were calculated at every third time step.[39] The data collected is 1.4 ps long. We further estimated the shear viscosity from the autocorrelation function of the off-diagonal elements of the stress tensor.

In the analysis, we used a geometrical criterion to assign the connectivity between different molecular motifs in the liquid.

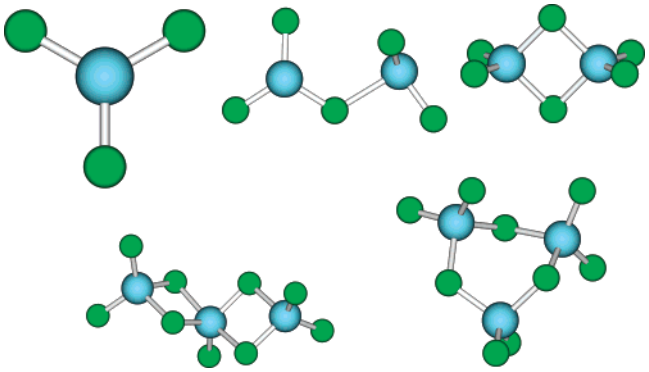

Figure 1. Calculated *n*-mers, $n = 2, 3$, as obtained from geometry optimization. First line: monomer, corner dimer, edge dimer; second line: edge trimer and corner trimer. The aluminum atoms are colored blue and the chloride atoms are colored green.

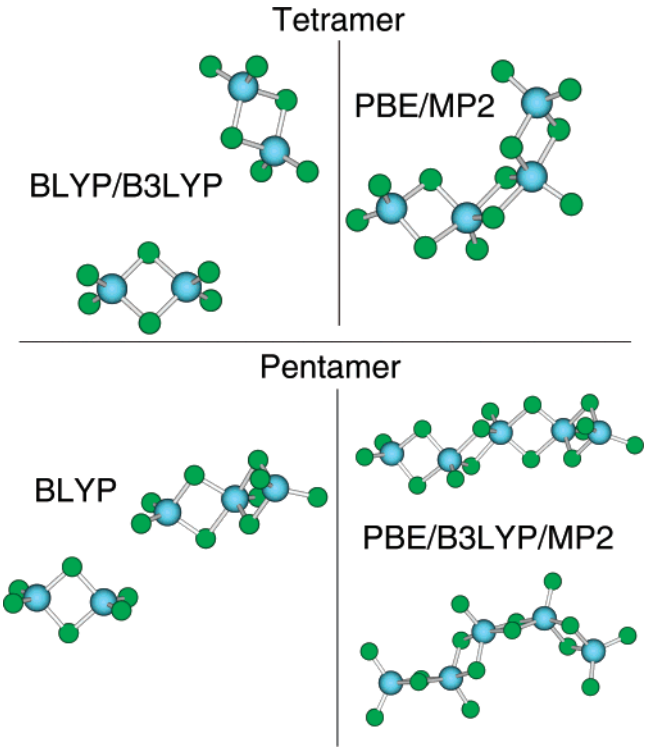

Figure 2. Tetramer and pentamer configurations for different methods.

An aluminum and chlorine atom were defined to be bound if the distance between them is at most 1.5 times the bond length in the $AlCl_3$ monomer, leading to a cutoff radius of 2.76 Å. Two Al atoms were regarded as belonging to the same cluster if they are linked with at least one Cl atom bound to both Al atoms by the criterion given above.

Average computer time for one Car−Parrinello molecular dynamics step on 32 CPUs of a IBM p690 was about 290 s during the BLYP run. Additional time needed for calculation of the maximally localized Wannier functions for the BLYP run was 310 s.

3. Small $[AlCl_3]_n$ Clusters via Static Calculations

3.1. Geometry and Energetics. In Figures 1 and 2, we depicted all *n*-mers as obtained from geometry optimizations for different methods. The smaller *n*-mers (Figure 1) turned out to be similar for all methods, but the tetramer and the pentamer showed different structures depending on the method. There are two well-known dimer configurations and two trimer

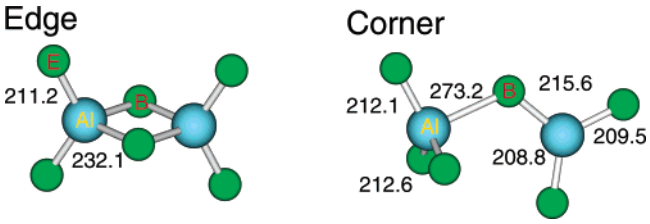

Figure 3. The two dimer conformers. Distances are given in pm and are obtained from the BLYP/TZVP calculations.

TABLE 1: Geometrical Parameters for the Two Dimers Obtained with Different Methods[a]

	BLYP	B3LYP	PBE	MP2	expt
r(Al−Al)$_{edge}$ (pm)	327	324	322	317	321
r(Al−E)$_{edge}$ (pm)	211	210	210	208	207
r(Al−B)$_{edge}$ (pm)	232	230	230	227	225
α(Al−B−Al)$_{edge}$ (deg)	89.6	89.6	88.7	88.6	91
r(Al−Al)$_{corner}$ (pm)	417	406	397	383	
r(Al−B)$_{corner}$ (pm)	273	265	259	250	
α(Al−B−Al)$_{corner}$ (deg)	116.6	115.6	113.2	111.1	

[a] Experimental values are taken from ref 11

configurations, i.e., either connected over an edge or through a corner atom, see Figure 1, first and second line.

Whereas the structures obtained with PBE and MP2 agree well in all the clusters studied, BLYP and B3LYP give different structures from them for the tetramer and BLYP for the pentamer. In the case of the tetramer, BLYP and B3LYP optimizes to separated edge-sharing dimers as opposed to the fully covalently connected MP2 and PBE structures. For the pentamer, only the BLYP calculation fails to yield a fully covalently connected structure, but the cluster splits into a trimer and a dimer; see the second line in Figure 2.

Figure 3 depicts the two dimer conformers with distances and angles from the BLYP/TZVP calculations. Table 1 lists geometry parameters as obtained by geometry optimizations from static quantum chemical calculations. The data are in accordance with ref 11, where Hartree−Fock calculations were done with a 6-31G* basis set. The values of Alvarenga and co-workers[11] are r(Al-E)$_{edge}$ = 208.3 pm, r(Al−B)$_{edge}$ = 228.9 pm, and the Cl−Al−Cl angle is 89.1°. The length of the covalent bonds vary within 6 pm between different methods used, except for the aluminum distances to the bridge atoms in the corner configurations, where they differ up to 35 pm. For all parameters, the PBE functional data compares best with the MP2 data.

As can be seen in Table 1 and Figure 3, there are three characteristic parameters to distinguish the two conformers. One of them is the Al−Al distance, which is much longer in the case of the corner conformer. There is one very large Al−Cl bond length in the corner dimer; it is a distance to the bridge atom, which we mark in Figure 3 with a capital B. Another good criterion to distinguish the two conformers is the Al−B−Al angle. It is smaller in the case of the edge dimer. This will assist us to distinguish the connectivity of the $AlCl_3$ unities in the dynamic simulations below. Although these criteria do not reveal which *n*-mer is dominant in the simulation, they are helpful in deciding which connectivity of the monomers is present. Experimental data is also given in Table 1 for the edge dimer. All methods compare well with experimental data. Whereas the direct Al−Cl-distance is best reproduced by MP2, the Al−Al-distance of PBE compares very well with experiment.

By turning to the dipole moments listed in Table 2, we find the largest dipole moment for the corner dimer, whereas the monomer and the edge dimer have zero dipole moment. Both

TABLE 2: Dipole Moment for the Different Molecules[a]

	BLYP	B3LYP	PBE	MP2
monomer	0	0	0	0
dimer$_{corner}$	3.63	3.88	4.09	4.40
dimer$_{edge}$	0	0	0	0
trimer$_{edge}$	0.19	0.15	0.25	0.29
trimer$_{corner}$	0.49	0.53	0.55	0.82
tetramer	0.07	0.18	0.60	0.35
pentamer	0.29	0.27	0.15	0.38

[a] All values are in Debye.

TABLE 3: Interaction Energy in kJ/mol

	BLYP	B3LYP	PBE	MP2
dimer$_{corner}$	16.0	24.1	36.4	34.9
dimer$_{edge}$	201.1	220.2	233.3	154.3
trimer$_{edge}$	219.2	246.3	292.8	258.3
trimer$_{corner}$	324.5	355.7	379.6	374.8
tetramer	404.0	431.5	377.9	321.4
pentamer	421.7	357.7	461.1	380.9

TABLE 4: Interaction Energy Per Monomer in kJ/mol

	BLYP	B3LYP	PBE	MP2
dimer$_{corner}$	8.0	12.0	18.2	17.5
dimer$_{edge}$	100.6	110.1	116.7	77.2
trimer$_{edge}$	73.1	82.1	97.6	86.1
trimer$_{corner}$	108.2	118.6	126.5	124.9
tetramer	101.0	107.9	94.5	80.4
pentamer	84.3	71.5	92.2	76.2

conformers of the trimer have a small dipole moment. For the one that is built by edge-connecting tetrahedra, the value is 0.2−0.3 D, and the trimer, which has the shape of a closed ring built up by corner-sharing tetrahedra, has also a dipole moment of about 0.5−0.8 D.

If we consider the two monomers in the configurations they hold in each dimer, we obtain a dipole moment of 2.64 D for each monomer in the edge, and 1.18 and 0.68 D in the corner conformer. Whereas the dipole moments of the monomer units in the edge-sharing dimer point in opposite directions and thus cancel each other, the ones in the corner sum up. From this information, we might be able to determine the way the monomer units are connected in the simulation. The higher clusters also show almost no total dipole moment, indicating that again the dipole moments of the monomer units cancel each other.

From the quantum chemical calculations, we also derived interaction energies.

Table 3 lists the interaction energy as obtained with the supramolecular approach, and Table 4 lists the interaction energy divided by the number of monomer units.

All methods show similar trends, but deviations between DFT methods and MP2 are up to 40 kJ/mol per monomer unit, see Table 4. For instance, the DFT-based methods overestimate the edge-sharing dimer interaction energy strongly compared to the MP2 value. In general, the corner configuration of the dimer is much weaker for all methods (16−35 kJ/mol) than the edge configuration (233−154 kJ/mol). This is not the case for the trimer; here, the corner-sharing configuration seems to be more stable (compare Table 3, fourth and fifth line). Altogether, the corner trimer is the most stable cluster per unit. The energy is increasing up to this trimer and then decreasing again. This might be comparable to hydrogen-bonded water clusters, where ring structures are often found to be more stable than chains or branched structures due to cooperative effects.[40]

3.2. Reactions. In standard textbooks, an enthalpy change of −124 kJ/mol for the reaction $2AlCl_3 \leftrightarrow Al_2Cl_6$ can be found.[4]

TABLE 5: Energies for the Reaction from Monomer to Dimer[a]

	$2AlCl_3 \rightarrow Al_2Cl_6^{corner/edge}$			
	BLYP	B3LYP	PBE	MP2
ΔD^{corner} (kJ/mol)	−7.3	−12.7	−24.0	−36.6
ΔD^{edge} (kJ/mol)	−80.8	−92.7	−114.1	−136.9
ΔD_0^{corner} (kJ/mol)	−5.5	−10.7		
ΔD_0^{edge} (kJ/mol)	−77.0	−88.7	−110.3	−132.8

[a] First line: reaction to edge; second line: reaction to corner.

TABLE 6: Thermochemistry for the Reaction from Corner to Edge Conformer for the Two Dimers and Different Methods

	$Al_2Cl_6^{corner} \rightarrow Al_2Cl_6^{edge}$			
	BLYP	B3LYP	PBE	MP2
ΔD (kJ/mol)	−73.5	−80.1	−90.0	−100.3
ΔD_0 (kJ/mol)	−71.5	−78.1	−88.1	−98.4
ΔS (J/(mol K))	−35.5	−32.8	−5.6	3.10
ΔG (kJ/mol)	−62.9	−70.3	−88.2	−101.1

Different energies are given in Table 5. The ΔD^{edge} data compares well to the value in the literature[10] of 72 kJ/mol.

Table 6 lists thermochemical data for the reaction from corner to edge with different methods. All methods favor energetically the edge conformer. The zero-point energy corrections lead only to minor changes in the values. Entropic contributions are calculated to be small, leading to an overall exergonic reaction with negative enthalpy ΔG. However, whereas the density functionals predict a negative entropic contribution, we find a positive (yet very small) value for MP2. As with several previously discussed properties, we find best agreement between the PBE functional and MP2 calculations.

4. Dynamical Studies

4.1. Isolated Dimer. In Figure 4, we depict the monomer dipole moment distribution from the simulations of the isolated units at 300 K. Whereas the monomer (around 1 D) and the edge-dimer (around 5 D) have a sharp distribution, the corner dimer provides values between 0 and 5 D with a maximum at about 2 D.

This will also help to distinguish both of the dimer configurations in the liquid. Neither the edge nor the corner dimer are unstable or transform into each other under temperature, although the edge conformer is by 60 kJ/mol more stable, which means that the transformation reaction must have a sustainable barrier.

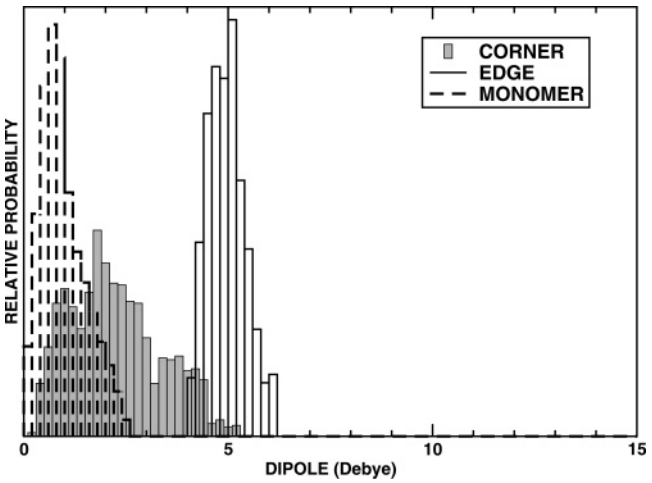

Figure 4. Monomer dipole distribution from a simulation of single molecules in a BLYP dynamical trajectory.

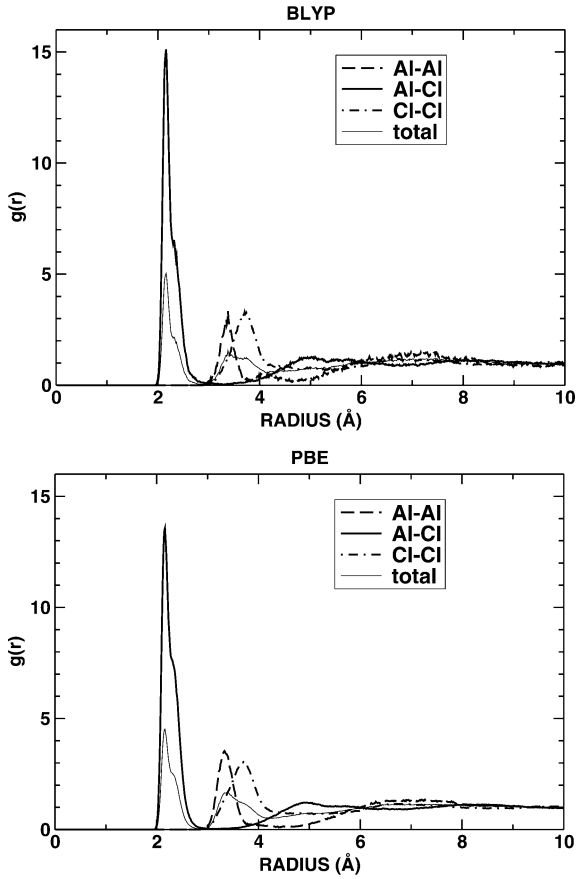

Figure 5. Partial and total radial pair distribution functions from the BLYP (top) and PBE (bottom) simulations.

4.2. The Structure of Liquid $AlCl_3$. Structural features of a liquid can be captured from the radial pair distribution function. In Figure 5, the radial pair distribution function for the BLYP and PBE run is depicted. Both simulations show similar curves for the pair functions. The functions for the BLYP run are less smooth due to shorter simulation time. In the following, we only will discuss the data from the PBE simulation, if not otherwise mentioned. There is a large peak indicating the intramolecular Al−Cl bond at approximately 214 pm in the Al−Cl function, see bold curve in Figure 5. A noticeable shoulder is also apparent at approximate 235 pm. This value corresponds to the distance between Al and the bridge Cl in the edge-sharing conformation of the dimer. Furthermore, the Al−Al function (dashed line Figure 5) shows the first peak around 328 pm, which is another attribute of the edge-sharing conformer. There might be also a very small amount of corner-sharing conformers present because the functions show a nonvanishing probability at 414 pm. However, on the basis of the radial pair distribution function along the simulation, this is not conclusive.

The Cl−Al−Cl angular distribution in Figure 6 proves the dominance of the edge-sharing over the corner-sharing dimer in our liquid. The majority of the units are connected via angles 80−100°, and only a small amount of units are connected with angles larger than this. Yet the liquid does not need to consist only of monomers and dimers. To further gain insight into the structural behavior, we considered with simple geometrical criteria, namely the Al−Al distance, the number of units that contribute to a cluster.

Figure 7 shows the relative number of molecules plotted against the length of chains. It is apparent that our liquid contains almost no monomers because the probability for the monomer is less than 0.05. This is also expected on energetic grounds,

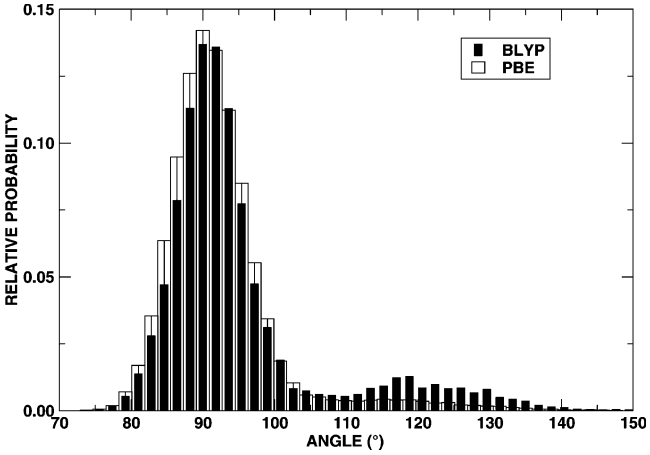

Figure 6. Cl−Al−Cl angular distribution in the dynamical simulations.

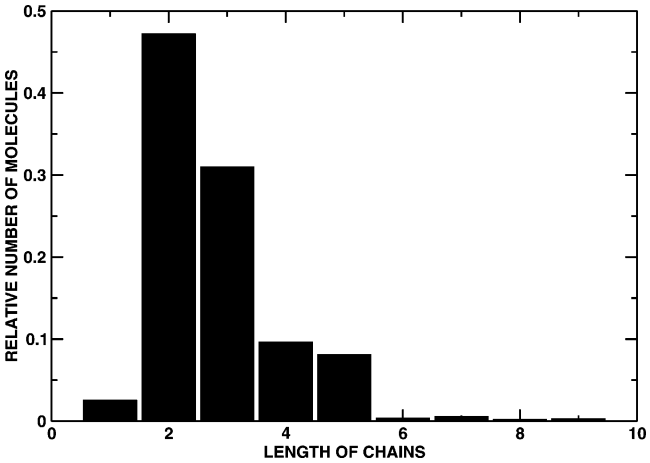

Figure 7. Relative distribution of different chain lengths in the PBE simulation.

see Table 3. The dimers are the most abundant species, followed by trimers. There are also 10% each of the tetramers and pentamers, but higher species such as hexamers become less probable. This also shows that a discussion of the condensed phase based on isolated clusters and their interaction energies only leads to wrong impressions. Instead, a quantum cluster equilibrium (QCE) approach or simulations are needed.[41−44] The interaction energies given in the previous section in Table 4 indicate that corner dimers should be the most present structural motif; however, in the simulations of the liquid-phase, dimers are more often observed than trimers. In general, we can say that most molecules are incorporated into clusters greater than the monomer and smaller than the hexamer.

To ensure that our sample is well equilibrated and to rule out a continuous transition in our simulation, we further analyzed all data in time domains of 1 ps. We saw no systematic trend along the simulation, i.e., the behavior in each time domain is the same.

Finally, we show the dipole moment distribution of the monomers in the liquid in Figure 8. We see a sharp peak around 4.5 D. A weak peak can be recognized at around 1.75 D and very low intensity of higher dipole moments. In the previous sections, we determined the dipoles of the optimized monomer and the monomers in the two dimer structures. We found that, in the edge dimer, the monomers establish higher dipole moments that must cancel each other, whereas the corner dimer (that itself has a high total dipole moment) exhibits smaller dipole moments in its monomer units. From this, we infer again that our liquid mainly consists of the edge-sharing structural

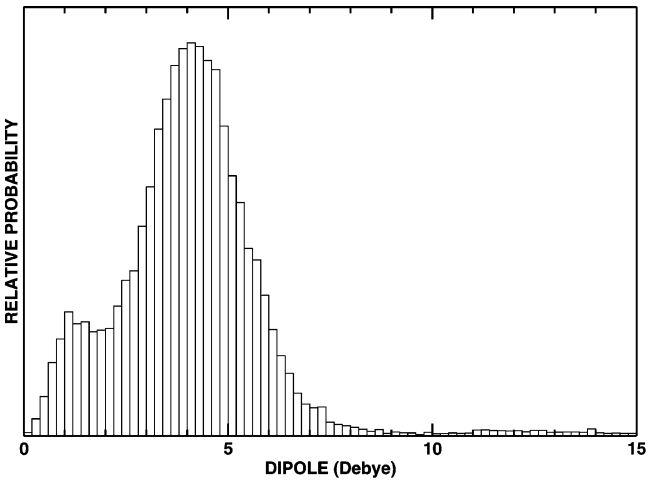

Figure 8. Distribution of monomer dipoles from a simulation of liquid $AlCl_3$ in the BLYP dynamical trajectory.

feature, but that, to a small extent, the other connectivity pattern is also populated. What is evident from the high dipole moments present in the dipole moment distribution in Figure 8 is that the liquid is sizably polarized.

For the viscosity of $AlCl_3$, we derive a value of 0.5 ± 0.2 mPI. The large error bars arise from the relatively small size of the sample and short simulation time. However, the value is in reasonable agreement with the value of 0.36 mPI reported in ref 45.

5. Summary

We have studied the properties of $AlCl_3$ via static electronic structure calculations of isolated clusters and by Car−Parrinello simulations of isolated clusters and of liquid $AlCl_3$.

Within the static electronic structure calculations, density functional theory was compared to MP2. Three different functionals were tested, namely the BLYP, the B3LYP, and the PBE functional. For the smaller clusters (up to three molecules), we found that all methods compare well in geometrical features. However, the systems calculated with BLYP and B3LYP rearranged upon optimization and did not yield a stable tetramer and pentamer, whereas PBE and MP2 compared well in the structure of those clusters. Furthermore, PBE gave energetic results close to MP2, whereas B3LYP and BLYP deviated more from MP2. Altogether we found a good agreement with calculations from literature.[11] We also found for all methods that the ring trimer connected via corners shows large cooperative effects compared to the corner and edge dimer. For all density functional calculations, the edge dimer is the second most stable structure (after the corner trimer), whereas MP2 also yields a more stable edge trimer and a more stable tetramer.

From comparison of the two dimers, characteristic geometrical parameters could be deduced. These were later used to detect structural motifs by analyzing the radial pair distribution functions and an angular distribution function. From the Al−Cl and the Al−Al radial pair distribution functions as well as from the angular distribution indications were found for the preference of edge-sharing units.

We further analyzed the Car−Parrinello trajectory with a simple geometrical criterion to detect different-sized clusters. We indeed found the dimer to be the most abundant species. Trimers are present up to 30%, whereas tetramers and pentamers are only present by 10%. Larger clusters were hardly found and monomers were also not present in our simulation of the liquid. This can not only be attributed to an inadequate description by

the employed approximations for the exchange-correlation functional in the density functional theory because all functionals gave a stronger trimer than dimer in accordance with MP2. This result is very important with regard to the fact that the liquid phase cannot be explained on the grounds of energetic discussions of isolated (static) clusters only. At least calculations of populations such as in a quantum cluster equilibrium approach are necessary.[41−44]

The dipole moments of the monomers in the dimers were analyzed and revealed that the monomer dipole moment is four times larger in the edge dimer than in the corner dimer, although the corner dimer itself has a higher dipole moment than the edge species. Again, for the purpose of comparison, we analyzed the isolated species, a monomer and two different dimers, but this time we ran Car−Parrinello simulations to obtain the local dipole moment of the monomer units within the clusters. Comparison of the results with the bulk liquid indicated again the presence of the edge dimer together with the fact that the bulk is highly polarized, and thus simulations with polarizable force fields or Car−Parrinello type simulations are necessary to represent this system.[10] However, all results point to the fact that there is also some small percentage of corner connectivity present that might be attributed to the most stable corner connected cluster, namely the trimer.

From this study, we have learned that liquid $AlCl_3$ is a sizably polarized liquid. It contains edge-connected dimers that are probably rather in concurrence to cooperative ring trimers connected via corners than to corner dimers. The insight gained from our simulations on $AlCl_3$ reported in this study will serve as a starting point for future simulations on ionic liquids derived from $AlCl_3$.

Acknowledgment. B.K. would like to express her gratitude for the generous allocation of computer time at the Rechenzentrum Karlsruhe and the Sonderforschungsbereich 624 for the financial resources. The program MOLDEN[46] has been used for the visualization of structures.

References and Notes

(1) Welton, T. *Chem. Rev.* **1999,** *99,* 2071.
(2) Dymek, C. J., Jr.; Williams, J. L.; Groeger, D. J.; Auborn, J. J. *J. Electrochem. Soc.* **1984,** *131,* 2887.
(3) Reynolds, G. F.; Dymek, C. J., Jr. *J. Power Sources* **1985,** *15,* 109.
(4) Holleman, A. F.; Wiberg, E. *Lehrbuch der Anorganischen Chemie;* Walter de Gruyter: Berlin, 1985.
(5) Badyal, Y. S.; Allen, D. A.; Howe, R. A. *J. Phys.: Condens. Matter* **1994,** *6,* 10193.
(6) Tosi, M. P. *J. Phys: Condens. Matter* **1994,** *6,* A13.
(7) Abramo, M. C.; Caccmo, C. *J. Phys.: Condens. Matter* **1994,** *6,* 4405.
(8) Fischer, W. *Z. Anorg. Chem.* **1931,** *200,* 340.
(9) Tanke, E. *Z. Anorg. Chem.* **1931,** *200,* 357.
(10) Hutchinson, F.; Walters, M. K.; Rowley, A. J.; Madden, P. A. *J. Chem. Phys.* **1999,** *110,* 5821.
(11) Alvarenga, A. D.; Saboungi, M.; Curtiss, L.; Grimsditch, M. *Mol. Phys.* **1994,** *81,* 409.
(12) Takahashi, S.; Curtiss, L. A.; Gosztola, D.; Koura, N.; Saboungi, M.-L. *Inorg. Chem* **1995,** *34,* 2990.
(13) Bernasconi, L.; Madden, P. A.; Wilson, M. *PhysChemComm* **2002,** *5,* 1.
(14) Pfleiderer, T.; Waldner, I.; Bertagnolli, H.; Tölheide, K.; Fischer, H. E. *Phys. Chem. Chem. Phys.* **2003,** *5,* 5313.
(15) Hutchinson, F.; Wilson, M.; Madden, P. A. *Mol. Phys.* **2001,** *99,* 811.
(16) Car, R.; Parrinello, M. *Phys. Rev. Lett.* **1985,** *55,* 2471.
(17) Takahashi, S.; Suzuya, K.; Kohara, S.; Koura, N.; Curtiss, L. A.; Saboungi, M.-L. *Z. Phys. Chem.* **1999,** *209,* 209.
(18) Ahlrichs, R.; Bär, M.; Häser, M.; Horn, H.; Kölmel, C. *Chem. Phys. Lett.* **1989,** *162,* 165.
(19) Becke, A. D. *Phys. Rev. A* **1988,** *38,* 3098.
(20) Lee, C.; Yang, W.; Parr, R. G. *Phys. Rev. B* **1988,** *37,* 785.
(21) Perdew, J. P.; Burke, K.; Ernzerhof, M. *Phys. Rev. Lett.* **1996,** *77,* 3865.
(22) Dunlap, B. I.; Connolly, J. W. D.; Sabin, J. R. *J. Chem. Phys.* **1979,** *71,* 3396.
(23) Ziegler, T.; Rauk, A.; Baerends, E. J. *Theor. Chim. Acta* **1977,** *43,* 261.
(24) Eichkorn, K.; Treutler, O.; Öhm, H.; Häser, M.; Ahlrichs, R. *Chem. Phys. Lett.* **1995,** *240,* 283.
(25) Becke, A. D. *J. Chem. Phys.* **1993,** *98,* 5648.
(26) Stephens, P. J.; Devlin, F. J.; Chabalowski, C. F.; Frisch, M. J. *J. Phys. Chem.* **1994,** *98,* 11623.
(27) Haase, F.; Ahlrichs, R. *J. Comput. Chem.* **1993,** *14,* 907.
(28) Schäfer, A.; Huber, C.; Ahlrichs, R. *J. Chem. Phys.* **1994,** *100,* 5829.
(29) Boys, S. F.; Bernardi, F. *Mol. Phys.* **1970,** *19,* 553.
(30) Neugebauer, J.; Reiher, M.; Kind, C.; Hess, B. A. *J. Comput. Chem.* **2002,** *23,* 895.
(31) CPMD V3.8; Copyright IBM Corp 1990−2003, Copyright MPI für Festkörperforschung Stuttgart 1997−2001; see also www.cmpd.org.
(32) Troullier, N.; Martins, J. L. *Phys. Rev. B* **1991,** *43,* 1993.
(33) Kleinman, L.; Bylander, D. M. *Phys. Rev. Lett.* **1982,** *48,* 1425.
(34) Nosé, S. *Mol. Phys.* **1984,** *52,* 255.
(35) Nosé, S. *J. Chem. Phys.* **1984,** *81,* 511.
(36) Hoover, W. G. *Phys. Rev. A* **1985,** *31,* 1695.
(37) Hoover, W. G. *Phys. Rev. A* **1985,** *31,* 1695.
(38) Martyna, G. J.; Hughes, A.; Tuckerman, M. E. *J. Chem. Phys.* **1999,** *110,* 3275.
(39) Marzari, N.; Vanderbilt, D. *Phys. Rev. B* **1997,** *56,* 12847.
(40) Ludwig, R. *Angew. Chem., Int Ed.* **2001,** *40,* 1808.
(41) Weinhold, F. *J. Chem. Phys.* **1998,** *109,* 367.
(42) Kirchner, B. *J. Chem. Phys.* **2005,** *123,* 204116.
(43) Ludwig, R.; Weinhold, F. *J. Chem. Phys.* **1999,** *110,* 508.
(44) Borowski, P.; Jaroniec, J.; Janowski, T.; Woliński, K. *Mol. Phys.* **2003,** *101,* 1413.
(45) Janz, G. J. *J. Phys. Chem. Ref. Data* **1988,** *17,* Suppl. 2.
(46) Schaftenaar, G.; Noordik, J. H. *J. Comput.-Aided Mol. Design* **2000,** *14,* 123.